



# Interrelation of EDXRF and comparator INAA to analyze REE mineral resources

I. Silachyov<sup>1</sup>

Received: 1 February 2024 / Accepted: 20 March 2024 / Published online: 15 April 2024  
© Akadémiai Kiadó, Budapest, Hungary 2024

## Abstract

Joint application of energy dispersive X-ray fluorescence analysis (EDXRF) and instrumental neutron activation analysis (INAA) was considered to determine the contents of sixteen rare earths elements (REE) in the corresponding mineral resources. K series of the majority of REEs was excited by the bremsstrahlung of the X-ray tube operating at accelerating voltage 70 kV, the modified version of a portable X-ray spectrometer is equipped with. A range of ore samples collected from three REE deposits of the Republic of Kazakhstan essentially differing in their elemental composition was investigated. A way of EDXRF and INAA optimum integration to analyze REE resources was proposed taking account of the advantages and drawbacks of both methods.

**Keywords** Rare earth elements · Mineral resources · X-ray fluorescence · Neutron activation analysis

## Introduction

In spite of the ongoing progress in analytical techniques for trace element determination [1], analysis of mineral resources for individual rare earth element (REE) content is still a difficult task. The problem is generally solved at present by the instrumental methods of elemental analysis, mainly by inductively coupled plasma optical emission spectrometry and mass spectrometry (ICP-OES and ICP-MS), atomic absorption spectrometry, instrumental neutron activation analysis (INAA) [2–4], and different variants of X-ray fluorescence analysis (XRF) [5].

If less-common electrothermal evaporation (ablation) of solid samples is not considered, main disadvantage of the first three methods lies in the necessity of sample dissolution [3, 6]. This presents a serious challenge for the analysis since REEs usually constitute firm natural compounds—silicates, oxides, sulphides, and phosphates. Various decomposition techniques are often selective, laborious and expensive; moreover they can not prevent samples from contamination by the reagents and do not ensure complete dissolution.

In this respect the nondestructive methods such as INAA and XRF can offer undoubted advantages. The first one still occupies a leading position in REE analysis [7] owing to a range of other favorable features too. The most important of them comprise minimum matrix effect, absence of the blank experiment, usually slight spectral interferences, high sensitivity and moderate cost of the analysis. These benefits promote broad application of INAA to analyze rocks, minerals, sediments and other geological objects for REE content [8–12]. The main drawbacks of INAA consist in a rather long time of all REE determination and in periodic technical inaccessibility of the research reactors (nuclear fuel replacement, and so on).

XRF is widely spread in elemental analysis of geological objects owing to its such advantages as promptness, simple sample preparation, and low cost. However, high-sensitive determination of lanthanides by XRF is seriously impeded by rather high values of their K-absorption edges (the minimum energies required for K series excitation) – from about 38.9 keV for La to approximately 63.3 keV for Lu [13]. That is why direct analysis of geological samples for REE contents by their K series by up-to-date energy dispersive XRF (EDXRF) spectrometers is practically unfeasible since they are most often equipped with X-ray tubes with Rh (Ag) anode or with W anode and a secondary target lighter than La.

✉ I. Silachyov  
silachyov@inp.kz

<sup>1</sup> Institute of Nuclear Physics, Ibragimov, Str.1,  
050032 Almaty, Republic of Kazakhstan

The task can be solved in principle using a standard radioisotope source for REE K series excitation. E.g., the common source  $^{241}\text{Am}$  (59.5 keV, quantum yield 35.9%, 10–20 mCi of the activity) makes possible rock analysis for La to Nd contents in case of counting of secondary X-rays by a Si semiconductor detector (SCD) [14]. Ge SCDs distinguished by their better detection efficiency of the high-energy X-rays additionally enable Sm and less often Gd determination in the objects characterised by REE contents close to their average values in the upper continental crust (UCC) [15]. If a much more active (1 Ci)  $^{241}\text{Am}$  source is used, Dy contents typical of common rocks can be determined too [16]. However, despite all its attractiveness, radioisotope excitation became of sporadic application in XRF lately due to availability of compact air-cooled X-ray tubes and to enhancement of legislation in the field of radioactive material turnover [17].

Comparative sensitivity of geological object analysis for REE contents is gained by wave dispersive XRF (WDXRF) spectrometers equipped with powerful (several kW) X-ray tubes for L series excitation. To deconvolve substantial spectral interferences of L lines extra efforts must be applied, usually with the help of linear regression analysis [18, 19]. WDXRF spectrometers reveal better resolution in the low-energy region than EDXRF ones enabling determination of all lanthanides, at least theoretically. In practice, unresolved superposition of REE L lines overlapping with the L lines of Ba and K lines of a matrix and minor elements from Ti to Zn presents a serious problem for rock analysis [5, 20]. That is why reliable determination of lanthanides by L series (both by WDXRF and EDXRF) still requires separation from matrix and preconcentration on a substrate [21], but the main advantages of XRF are lost then. Therefore this approach is far less developed at present comparing with the other destructive plasma-based techniques.

Different variants of XRF and INAA are well known to complement excellently one another in the study of rocks and similar objects [22–26] successfully competing together with ICP-MS in respect of accuracy and sensitivity of the analysis. Combining XRF and INAA, special interest is aroused if REEs should be basically determined, e.g. in the course of corresponding deposit explorations [27], developing the technologies of REE recovery from industrial wastes [28], or analyzing the non-traditional REE resources extremely resistant to chemical decomposition [29]. Studying uranium-rich samples, role of XRF greatly enhances since it makes possible to determine La, Ce, Nd, and Ho hardly accessible to INAA in this case due to severe spectral interferences caused by U fission products [30, 31].

Lately highly sensitive EDXRF is being used actively for prompt evaluation of Y and light lanthanides from La to Nd (and sometimes Sm) in different geological objects at the levels of their average UCC contents by exciting K series of

these elements by a low-power X-ray tube [32]. Sc and the heavier lanthanides are determined by INAA in the separate samples, if needed.

The present work continues the study of joint application of EDXRF and the internal standard based comparator INAA expanded to analyze REE mineral resources. Comparing with rock investigation, determination of Pr, Dy and Er by their short-lived radionuclides was added. Owing to REE increased contents, Gd became accessible by a low-energy gamma-line of the daughter radionuclide of  $^{161}\text{Gd}$  using a planar type SCD. The range of the lanthanides determined by EDXRF was also extended. To find the way of optimum combination of the methods a number of ore samples collected from three different type REE deposits of the Republic of Kazakhstan was analyzed for the contents of all REEs.

## Experimental

The samples of REE ores were prepared both for EDXRF and INAA in the same standard manner including grinding with a FRITSCH planetary mill PULVERISETTE 6 (Germany) to the particle size  $<0.071$  mm controlled with the help of a corresponding FRITSCH sieve.

To conduct EDXRF, approximately 15 g of the assays were pressed manually in aluminium dishes with Mylar film bottoms to provide the “saturated layer geometry”. Element content of the samples including Y, lanthanides, and Fe was determined with a portable X-ray spectrometer—modified version of RLP-21T (LLP “AspapGeo”, Almaty, Kazakhstan). The samples were measured for 30–60 min each and interpreted automatically in the real-time operation mode. Values of Fe mass fraction were used as the internal standard to determine other elements of interest by comparator INAA [22, 30–32]. Mn contents varying in different samples within more than one order of magnitude were determined too since conducting INAA by the short-lived radionuclides these values affected the decay time of the irradiated assays.

Modified RLP-21T presents the next generation of the corresponding model series of laboratory X-ray spectrometers specially designed to analyze powdered geological samples for lanthanide contents. Based on the commercial availability of the reliable portable X-ray tubes, the spectrometer is equipped with a low-power (10 W) one with a tungsten anode operating at accelerating voltage 70 kV. No intermediate target is used due to a drastic loss of the intensity of the primary X-rays. Characteristic fluorescence of an assay is excited by the X-ray tube bremsstrahlung. This makes possible to determine high-Z elements from Sn to Nd (or Sm) by their K series at the levels of their average UCC contents. The range of determined lanthanides is broadened to Er in rich REE ores and can include Yb in REE concentrates. The spectra are counted by a Peltier-cooled Si drift SCD, 25 mm<sup>2</sup>

**Table 1** Spectral interferences of the lanthanide X-ray lines (K series)

| Element | Line            | Energy, keV | Relative intensity, % | Spectral interference | Line            | Energy, keV     | Relative intensity, % |    |                 |       |    |
|---------|-----------------|-------------|-----------------------|-----------------------|-----------------|-----------------|-----------------------|----|-----------------|-------|----|
| Pr      | K <sub>α1</sub> | 36.03       | 100                   | Ba                    | K <sub>β3</sub> | 36.30           | 10                    |    |                 |       |    |
|         |                 |             |                       |                       | K <sub>β1</sub> | 36.38           | 18                    |    |                 |       |    |
| Nd      | K <sub>α1</sub> | 37.36       | 100                   | Ba                    | K <sub>β2</sub> | 37.26           | 6                     |    |                 |       |    |
| Sm      | K <sub>α2</sub> | 39.52       | 55                    | Ce                    | K <sub>β1</sub> | 39.26           | 19                    |    |                 |       |    |
| Eu      | K <sub>α2</sub> | 40.90       | 56                    | Pr                    | K <sub>β3</sub> | 40.65           | 10                    |    |                 |       |    |
|         |                 |             |                       |                       | K <sub>β1</sub> | 40.75           | 19                    |    |                 |       |    |
| Gd      | K <sub>α1</sub> | 41.54       | 100                   | Pr                    | K <sub>β2</sub> | 41.77           | 6                     |    |                 |       |    |
|         |                 |             |                       |                       | K <sub>α2</sub> | 42.31           | 56                    | Nd | K <sub>β3</sub> | 42.17 | 10 |
|         |                 |             |                       |                       |                 |                 |                       |    | K <sub>β1</sub> | 42.27 | 19 |
| Dy      | K <sub>α1</sub> | 43.00       | 100                   | Nd                    | K <sub>β2</sub> | 43.34           | 6                     |    |                 |       |    |
|         |                 |             |                       |                       | K <sub>α2</sub> | 45.21           | 56                    | Sm | K <sub>β3</sub> | 45.29 | 10 |
| Ho      | K <sub>α2</sub> | 46.70       | 56                    | Sm                    |                 |                 |                       |    | K <sub>β1</sub> | 45.41 | 19 |
|         |                 |             |                       |                       | Eu              | K <sub>β2</sub> | 46.58                 | 6  |                 |       |    |
|         |                 |             |                       |                       |                 | K <sub>β3</sub> | 46.90                 | 10 |                 |       |    |
| Er      | K <sub>α2</sub> | 48.22       | 56                    | Eu                    | K <sub>β2</sub> | 48.26           | 6                     |    |                 |       |    |
| Yb      | K <sub>α1</sub> | 52.39       | 100                   | Dy                    | K <sub>β1</sub> | 52.12           | 20                    |    |                 |       |    |

of the area, with an energy resolution 140 eV at the 5.9 keV line. A high efficiency spectra treatment algorithm is applied to find X-ray peak areas under the unfavourable values of signal-to-background ratio for the majority of lanthanides caused by the intense bremsstrahlung. All characteristic lines of both K and L series (5 and 19 lines, respectively) of every analyzed element are used by the software to approximate the spectra. To calculate element contents of the samples, a reference-free modified version of the “fundamental parameters method” is employed.

Table 1 presents spectral interferences of the main analytical lines K<sub>α1</sub> and K<sub>α2</sub> of the lanthanides [33] considering degradation of SCD energy resolution for higher energies.<sup>1</sup> K<sub>α</sub> lines never overlap one with another but only with the far less intensive K<sub>β</sub> lines of the lighter elements. Taking light to heavy lanthanide fractionation similar to that of typical rocks, the following interferences are the most significant: Pr can complicate Eu determination, Nd – determination of Gd. Sm impedes Dy evaluation to a smaller extent since only one K<sub>α2</sub> line of Dy is overlapped. Very high Ba mass fractions, exceeding that of Pr and Nd by a factor of twenty and more noticeably complicate determination of these elements; however, this can take place only if Pr and Nd contents are close to their average UCC values [32]. Other interferences in Table 1 are practically insignificant. Anyway, overlapping of lanthanide K lines is not so dramatic as L lines demonstrate and is far more precisely accounted by the software.

Unlike automatic control of the maximum count rate in RLP-21T by altering X-ray tube current, to avoid analyzer overload in INAA resulting in SCD energy resolution degradation, masses of REE ore assays  $m$  and irradiation time  $t_{irr}$  were specially selected empirically for the predetermined counting geometries based on the previous investigations. Considering the REE contents of the samples varied very significantly, expressing irradiation conditions using  $m t_{irr}$  product (mg h) seems more representative. In case of prolonged irradiation this value differed for different assays by a factor of 30 and more; the details are revealed below.

The assays taken with a Mettler Toledo analytical balance up to the fourth decimal ( $\pm 0.1$  mg) were prepared for irradiation following the routine procedure previously used for rock analysis [30–32]. Besides the investigated assays, every package included zirconium monitor ( $\approx 20$  mg of ZrO<sub>2</sub>) in the middle to evaluate epithermal to thermal neutron flux ratio  $1/f$  and the assays of chemically pure iron<sup>2</sup> ( $\approx 10$  mg) to determine Fe content of the samples more precisely, if it was lower 1% by EDXRF. Sometimes Fe assays acted as the external standard in comparator INAA when the investigated ones were drastically reduced in mass to avoid overirradiation or/and neutron flux self-shielding. The assays presenting different objects (REE ore deposits) were irradiated separately.

The ready packages wrapped in Al foil were placed in the position №4 inside peripheral vertical channel №10–6 of the

<sup>1</sup> The values assessed with the help of pure chemicals amounted  $\approx 340$  eV for K<sub>α1</sub> line of Pr and  $\approx 380$  eV for K<sub>α1</sub> line of Er.

<sup>2</sup> CRM GSO1634, the Institute of Reference Materials, Ekaterinburg, Russian Federation,  $98.2 \pm 0.1$  wt% of Fe.

light-water research reactor WWR-K, Institute of Nuclear Physics (INP), Almaty, in such a way that flat polyethylene bags containing assays were perpendicular to the channel axis. This allowed to minimize the influence of the gradient of neutron spectrum composition since its radial component (8.5% per 1 cm) was the same for all the assays and the axial one (1.2% per 1 cm) can be regarded negligible. Neutron flux gradient was accounted for every assay using the internal standard method. The thermal neutron ( $< 0.625$  eV) flux density in the channel was  $8.9 \cdot 10^{13} \text{ cm}^{-2} \text{ s}^{-1}$ , while the fast neutron (0.1–1.15 MeV) one amounted to  $6.0 \cdot 10^{12} \text{ cm}^{-2} \text{ s}^{-1}$  [29]. Spectrum composition of the neutron flux assessed for a range of irradiations by the “bare bi-isotopic method” [34, 35] was within  $1/f = 0.024\text{--}0.028$ .

To analyze the samples for Pr, Dy and Er contents the automated pneumatic transport system (PTS) was used [36] with the irradiation terminal installed in a horizontal channel of WWR-K. 50–100 mg of the assays were sealed in small flat polyethylene bags and fixed in HDPE transport capsules across the neutron flux. The capsules were irradiated one by one for 1–5 min by the thermal neutron flux density  $n \cdot 10^{12} \text{ cm}^{-2} \text{ s}^{-1}$ . Irradiation time was also selected empirically to provide maximum count rate of the analyzer, i.e. dead time about 30%. Since the PTS irradiation terminal abuts on the reactor tank from the outside, the neutron flux in it is more thermalized than in the peripheral channels:  $1/f = 0.012 \pm 0.001$ .

Most of the gamma-spectrometric measurements by the long-lived radionuclides, as well as by the short-lived ones, were carried out using an analytical complex consisting of an extended-range coaxial SCD GX5019 (Canberra, relative efficiency is 50% and an energy resolution is 1.86 keV at the 1332 keV peak of  $^{60}\text{Co}$ ) and a Canberra multi-channel analyzer DSA-1000. In the first case the assays were counted twice after 7–8 days of the decay time to determine La, Sm, Yb, and Lu, then after 3 weeks to analyze for Ce, Nd, Eu, Tb, Tm, and Sc contents. Counting time and geometry were 20 min and 60 mm to the detector cap, then about 40 min and 24 mm, respectively.

Count rates of the short-lived radionuclides  $^{142}\text{Pr}$ ,  $^{165}\text{Dy}$ , and  $^{171}\text{Er}$  were measured after 16–18 h of decay to allow  $^{56}\text{Mn}$  (worsening sensitivity of Er determination due to its intensive Compton continuum) decay to a reasonable activity. Just before counting the samples were taken from the transport capsules and placed above the detector cap, 24 mm distant. The counting time amounted to 2–5 h depending on the sensitivity of  $^{142}\text{Pr}$  determination, the worst of all under such conditions. La contents of the assays measured by INAA before were used as the internal standard [29].

Ho and Gd contents of the samples were determined with the help of another complex including a planar type SCD GLP36360 (ORTEC, the crystal dimensions are  $36 \times 13$  mm, an energy resolution is 585 eV at the 122 keV line of  $^{57}\text{Co}$ )

and a multi-channel analyzer DSPEC LF of the same manufacturer. The assays were counted for 40–60 min after 7 days of decay at the distance of 40 mm from the detector cap and then after 12 days, 10 mm distant, to analyze for Ho and Gd contents, respectively. Due to a higher energy resolution the planar SCD is being used routinely to determine Ho beginning from the mass fractions close to its average UCC quantity [31, 32]. Moreover, increased contents of lanthanides in REE resources enable to determine Gd by a low-energy gamma-line of  $^{161}\text{Tb}$ —the daughter radionuclide of  $^{161}\text{Gd}$  (see Table 2 below) [29, 30], despite GLP36360 has far less absolute detection efficiency than GX5019. Overall duration of REE determination doesn't exceed 3 weeks mentioned above.

Both SCDs were calibrated for relative detection efficiency using a multi-gamma ray standard MGS-1 ( $^{152}\text{Eu}$ ,  $^{154}\text{Eu}$ ,  $^{155}\text{Eu}$ ) by Canberra. To extend GLP36360 calibration curve to the lower energies an isotopic source  $^{133}\text{Ba}$  (Canberra) was added. Fourth power polynomials were used to approximate calibration functions. The calibration curve trend of GLP36360 and some more details of its calibration can be seen in [35].

MAESTRO software was used to collect gamma-ray spectra by the planar type SCD and GENIE 2000—by the coaxial one. Spectra treatment was carried out by “Anal-Gamma” software developed in INP. More information concerning treatment of gamma-ray spectra to calculate count rates of analytical peaks can be found in [37].

Main data relating application of the internal standard based INAA to analyze the samples for REE contents are compiled in Table 2. Only one analytical gamma-line of each radionuclide was used; if more lines are appropriate, the selected lines generally correspond to the recommended ones [7].

Besides Fe as the internal comparator mentioned above, Table 2 includes Th occasionally used with the same aim in view to determine Ho (or Ho and Gd), if  $^{59}\text{Fe}$  count rate by GLP36360 was too low. Th content of such samples was found using GX5019. If the analyzed radionuclides relate to the uranium fission products ( $^{40}\text{La}$  and others,  $U(n, f)$  denotes an interference), the corresponding contribution to their count rates was considered as usual [29].  $^{133}\text{Xe}$  being of the same origin was accounted as a spectral interference where necessary.  $^{133}\text{Xe}$  is not resolved reliably with  $^{166}\text{Ho}$  by a planar type SCD, so the count rate of the latter was found analytically by the results of two measurements, the second was a week later [29]. In the case of thorium high contents exceeding that of terbium by more than one order of magnitude,  $^{160}\text{Tb}$  was accounted for a  $^{233}\text{Pa}$  gamma-line. As the last resort GLP36360 was used to resolve  $^{160}\text{Tb}$  and  $^{233}\text{Pa}$  gamma-lines. Moreover, if the ratio of thorium to dysprosium mass fractions reached several times, contribution of a  $^{233}\text{Pa}$  X-ray line ( $K_{\alpha 2}$ ) was accounted too. This correction to

**Table 2** Main nuclear parameters and interferences of the radionuclides used to determine REEs by comparator INAA

| Radionuclide                           | Half-life, days | Energy, keV | Quantum yield, % | Interferences                         | Energy, keV    | Quantum yield, % | Detector |
|--|-----------------|-------------|------------------|---------------------------------------|----------------|------------------|----------|
| <sup>46</sup> Sc                       | 83.8            | 889.28      | 99.9             | –                                     | –              | –                | GX5019   |
| <sup>140</sup> La                      | 1.68            | 1596.2      | 95.4             | U( <i>n, f</i> )                      | –              | –                | GX5019   |
| <sup>141</sup> Ce                      | 32.5            | 145.44      | 48.3             | U( <i>n, f</i> )<br><sup>175</sup> Yb | –<br>144.86    | –<br>0.672       | GX5019   |
| <sup>142</sup> Pr                      | 0.797           | 1575.6      | 3.70             | –                                     | –              | –                | GX5019   |
| <sup>147</sup> Nd                      | 11.0            | 91.11       | 28.1             | U( <i>n, f</i> )                      | –              | –                | GX5019   |
| <sup>153</sup> Sm                      | 1.94            | 69.67       | 4.73             | <sup>187</sup> W<br><sup>140</sup> La | 69.31<br>68.92 | 3.17<br>0.075    | GX5019   |
| <sup>152</sup> Eu                      | 4943            | 121.78      | 28.7             | –                                     | –              | –                | GX5019   |
| <sup>161</sup> Tb ( <sup>161</sup> Gd) | 6.89            | 25.65       | 23.2             | <sup>122</sup> Sb                     | 25.27          | 0.950            | GLP36360 |
| <sup>160</sup> Tb                      | 72.3            | 298.58      | 26.1             | <sup>233</sup> Pa                     | 298.81         | 0.088            | GX5019   |
| <sup>165</sup> Dy                      | 2.3 h           | 94.70       | 3.80             | <sup>233</sup> Pa                     | 94.65          | 10.56            | GX5019   |
| <sup>166</sup> Ho                      | 1.12            | 80.57       | 6.71             | <sup>133</sup> Xe                     | 81.00          | 36.9             | GLP36360 |
| <sup>171</sup> Er                      | 7.5 h           | 308.29      | 64.0             | –                                     | –              | –                | GX5019   |
| <sup>170</sup> Tm                      | 128.6           | 84.25       | 2.48             | <sup>182</sup> Ta                     | 84.68          | 2.65             | GX5019   |
| <sup>175</sup> Yb                      | 4.18            | 396.33      | 13.2             | <sup>140</sup> La                     | 397.52         | 0.073            | GX5019   |
| <sup>177</sup> Lu                      | 6.65            | 208.37      | 10.4             | <sup>176</sup> Yb → <sup>177</sup> Lu | 208.37         | 10.4             | GX5019   |
| <sup>59</sup> Fe                       | 44.5            | 1099.2      | 56.5             | –                                     | –              | –                | GX5019   |
|  |                 | 192.34      | 3.08             | –                                     | –              | –                | GLP36360 |
| <sup>233</sup> Pa ( <sup>233</sup> Th) | 27.0            | 311.90      | 38.5             | –                                     | –              | –                | GX5019   |

<sup>165</sup>Dy count rate which usually never takes place appeared as a result of the long decay time optimized to determine Pr and Er. <sup>153</sup>Sm was determined by its the lower-energy gamma-line to avoid interference with <sup>233</sup>Pa, despite potential contribution of <sup>140</sup>La and <sup>187</sup>W accounted by the software which is usually quite small. A low-intensity <sup>140</sup>La gamma-line can overlap the analytical line of <sup>175</sup>Yb only in the cases of high fractionation of light to heavy lanthanide, when the ratio of La to Yb contents approaches 100; this possible interference is usually resolved by the software. Contribution of <sup>176</sup>Yb to the count rate of <sup>177</sup>Lu due to the (*n, γ*) reaction was evaluated using the basic equation of neutron activation [7]. Taking Yb to Lu relation equal to their average crustal ratio [38], a systematic addition to <sup>177</sup>Lu activity after 1 h irradiation for the richest ore samples doesn't exceed ≈2.2% and can be neglected comparing with the other sources of uncertainty. Moreover, this addition diminishes with *t<sub>irr</sub>* due to a far shorter half-life of <sup>177</sup>Yb (1.91 h) comparing with that of <sup>177</sup>Lu. Other interferences were insignificant and hence were ignored or resolved by the software.

## Results and discussion

Element content of the samples (*C<sub>a</sub>*) by INAA was determined using a modified equation of the simple comparator method of standardization [29]. The equation includes

*k*<sub>0</sub>-factors relatively to 411.8 keV gamma-line of radionuclide <sup>198</sup>Au for the analytical gamma-lines of the analyzed elements and the comparator [39] and the empirical correction factor *K<sub>a,c</sub>*. The latter takes account of the deviation of the used model from the avowed *k*<sub>0</sub>-method [40] and some other reasons. *K<sub>a,c</sub>* values, estimated earlier for every counting geometry of the both SCDs with the help of multielement CRMs, are used ever since in all investigations.

There is no a *k*<sub>0</sub>-factor for radionuclide <sup>161</sup>Tb (Table 2) in the database [39], so *k*-factor was taken instead as the product of the corresponding nuclear constants [35]:

$$k = \sigma_0 \theta P_\gamma M^{-1}, \quad (1)$$

where  $\sigma_0$  is thermal neutron cross-section (cm<sup>2</sup>),  $\theta$  is isotopic abundance (%),  $P_\gamma$  is the quantum yield of the measured gamma-line (%),  $M$  is the atomic mass (Da). All nuclear constants except for  $P_\gamma$  relate to the activated short-lived radionuclide <sup>160</sup>Gd,  $P_\gamma$  – to the gamma-line of its daughter long-lived <sup>161</sup>Tb (25.7 keV).

Correction for the analytical gamma-ray self-absorption was carried out in the cases when mass or major element composition of the assays were noticeably different from that typical of the CRM assays used for *K<sub>a,c</sub>* evaluation (50–100 mg and light aluminosilicate matrix). Actually, only the gamma-line of <sup>161</sup>Tb was touched on. Using the approximation of the “thin irradiating layer” [41]

**Table 3** REE and some other element contents of OREAS 460 by EDXRF and INAA,  $\mu\text{g g}^{-1}$  ( $P=0.95$ )

| Element | Certified value | Measured value |             | $E_n$ -score |       |
|---------|-----------------|----------------|-------------|--------------|-------|
|         |                 | EDXRF          | INAA        | EDXRF        | INAA  |
| Sc      | 27.9±0.8        | –              | 29.5±2.8    | –            | 0.55  |
| Y       | 60±2            | 61±13          | –           | 0.08         | –     |
| La      | 1369±43         | 1430±200       | 1380±120    | 0.32         | 0.09  |
| Ce      | 1798±44         | 1880±200       | 1790±160    | 0.40         | –0.05 |
| Pr      | 244±5           | 243±48         | 238±23      | –0.02        | –0.25 |
| Nd      | 781±28          | 800±100        | 805±75      | 0.23         | 0.30  |
| Sm      | 107±2           | 107±23         | 108±10      | 0            | 0.10  |
| Eu      | 22.7±0.6        | 21.6±8.3       | 23.0±2.0    | –0.13        | 0.14  |
| Gd      | 50±2            | 54±13          | 47.6±4.8    | 0.30         | –0.56 |
| Tb      | 4.84±0.12       | –              | 4.70±0.43   | –            | –0.31 |
| Dy      | 19.8±0.5        | 18.7±4.4       | 19.5±2.0    | –0.25        | –0.15 |
| Ho      | 2.77±0.13       | –              | 2.9±0.4     | –            | 0.31  |
| Er      | 6.01±0.18       | –              | 6.6±1.1     | –            | 0.53  |
| Tm      | 0.70±0.03       | –              | 0.68±0.10   | –            | –0.19 |
| Yb      | 3.91±0.14       | –              | 3.88±0.39   | –            | –0.07 |
| Lu      | 0.52±0.03       | –              | 0.515±0.052 | –            | –0.08 |
| Th      | 116±2           | –              | 117±10      | –            | 0.10  |
| U       | 4.21±0.10       | –              | 4.40±0.80   | –            | 0.24  |
| Fe, %   | 18.90±0.42      | 19.22±0.45     | –           | 0.52         | –     |

correction for photoelectric absorption and scattering of 25.7 keV gamma-line didn't exceed several percents.

To assess thermal and resonance neutron self-shielding by the samples a spreadsheet by Chilian C, et al. [42] was applied. With 50–100 mg assays the corresponding correction is  $\leq 1\%$  while Sm, Eu, and Gd contents don't exceed their 20-fold percentage in UCC. Thermal neutron self-shielding was accounted mainly by using Fe (and La) as the internal standard where possible. If Th was used in this end in view, and to avoid corrections for resonance neutron self-shielding following any model [43], assay masses were reduced to the sizes securing a negligible influence of the effect as shown below.

To assess EDXRF and INAA by the sensitivity and accuracy of the results implying their further combination, several CRMs of REE ores were investigated at first: OREAS 460 and OREAS 100a by Ore Research & Exploration (Australia) and OSO 528 by the All-Russian Scientific Research Institute of Mineral Resources (Moscow). High mass fractions of the light lanthanides in the first CRM (Carbonatite supergene REE-Nb ore) reaching  $\approx 30$  crust average values for La, Ce and Nd gradually decrease to the common contents in rocks for the heaviest REEs. The other two CRMs (Uranium-bearing ore and Phosphorus rare earth uranium ore, respectively) are characterized by the increased mass fractions of the heavier lanthanides comparing with the lighter ones. The CRM assays were prepared and analyzed by both methods as mentioned above.

The results of CRM analyses for REE and Fe contents by EDXRF are presented in Tables 3, 4, 5) with their 95% confidence limits. Sc can't be determined reliably since its

**Table 4** REE and some other element contents of OREAS 100a by EDXRF and INAA,  $\mu\text{g g}^{-1}$  ( $P=0.95$ )

| Element | Certified value | Measured value |           | $E_n$ -score |       |
|---------|-----------------|----------------|-----------|--------------|-------|
|         |                 | EDXRF          | INAA      | EDXRF        | INAA  |
| Sc      | 6.10            | –              | 6.71±0.60 | –            | –     |
| Y       | 142±3           | 133±23         | –         | –0.39        | –     |
| La      | 260±9           | 271±48         | 268±23    | 0.23         | 0.32  |
| Ce      | 463±20          | 454±48         | 457±40    | –0.17        | –0.13 |
| Pr      | 47.1±2.4        | 44.5±8.3       | 48.9±4.9  | –0.30        | 0.33  |
| Nd      | 152±8           | 143±23         | 149±13    | –0.37        | –0.20 |
| Sm      | 23.6±0.4        | 22.0±8.3       | 24.7±2.1  | –0.19        | 0.51  |
| Eu      | 3.71±0.23       | –              | 3.74±0.31 | –            | 0.08  |
| Gd      | 23.6±1.4        | 23.3±8.3       | 23.8±2.4  | –0.04        | 0.07  |
| Tb      | 3.80±0.23       | –              | 3.76±0.34 | –            | –0.10 |
| Dy      | 23.2±0.4        | 23.0±8.3       | 23.4±2.3  | –0.02        | 0.09  |
| Ho      | 4.81±0.14       | –              | 4.87±0.58 | –            | 0.10  |
| Er      | 14.9±0.5        | 17.3±4.4       | 15.4±1.6  | 0.54         | 0.30  |
| Tm      | 2.31±0.11       | –              | 2.29±0.22 | –            | –0.08 |
| Yb      | 14.9±0.4        | –              | 15.9±1.4  | –            | 0.69  |
| Lu      | 2.26±0.11       | –              | 2.33±0.21 | –            | 0.30  |
| Th      | 51.6±2.7        | –              | 51.4±5.1  | –            | –0.03 |
| U       | 135±7           | –              | 126±11    | –            | –0.69 |
| Fe, %   | 4.66±0.06       | 4.72±0.17      | –         | 0.33         | –     |

**Table 5** REE and some other element contents of OSO 528 by EDXRF and INAA,  $\mu\text{g g}^{-1}$  ( $P=0.95$ )

| Element | Certified value | Measured value |             | $E_n$ -score |       |
|---------|-----------------|----------------|-------------|--------------|-------|
|         |                 | EDXRF          | INAA        | EDXRF        | INAA  |
| Sc      | 15.7 ± 1.5      | –              | 15.9 ± 1.5  | –            | 0.09  |
| Y       | 603 ± 59        | 600 ± 100      | –           | –0.05        | –     |
| La      | 444 ± 33        | 456 ± 48       | 460 ± 40    | 0.21         | 0.31  |
| Ce      | 782 ± 69        | 750 ± 100      | 768 ± 70    | –0.26        | –0.14 |
| Pr      | 87.0 ± 3.4      | 84 ± 13        | 89.1 ± 8.9  | –0.22        | 0.22  |
| Nd      | 382 ± 25        | 367 ± 48       | 382 ± 32    | –0.28        | 0     |
| Sm      | 82.1 ± 4.0      | 89 ± 13        | 83.9 ± 6.8  | 0.51         | 0.23  |
| Eu      | 21.7 ± 0.5      | 20.1 ± 8.3     | 22.4 ± 1.8  | –0.38        | 0.37  |
| Gd      | 100.2 ± 5.9     | 108 ± 23       | 102 ± 10    | 0.33         | 0.16  |
| Tb      | 15.1 ± 0.4      | 17.0 ± 4.4     | 15.2 ± 1.3  | 0.43         | 0.07  |
| Dy      | 89.7 ± 3.2      | 88 ± 13        | 86.6 ± 8.7  | –0.13        | –0.33 |
| Ho      | 18.5 ± 0.7      | 21.0 ± 8.3     | 18.8 ± 1.8  | 0.30         | 0.16  |
| Er      | 51.2 ± 0.9      | 51 ± 13        | 51.5 ± 5.2  | –0.02        | 0.06  |
| Tm      | 6.68 ± 0.30     | –              | 6.70 ± 0.65 | –            | 0.03  |
| Yb      | 40.2 ± 0.6      | –              | 41.2 ± 3.9  | –            | 0.25  |
| Lu      | 5.64 ± 0.23     | –              | 5.81 ± 0.48 | –            | 0.32  |
| Th      | –               | –              | 9.57 ± 0.80 | –            | –     |
| U       | 376 ± 13        | –              | 365 ± 33    | –            | –0.31 |
| Fe, %   | 15.33           | 15.53 ± 0.45   | –           | –            | –     |

$K_{\alpha}$  line is always completely overlapped by the far more intensive (by several orders of magnitude)  $K_{\beta}$  line of Ca. Lu is inaccessible as a rule because the tube accelerating voltage is not high enough to excite efficiently its K series by the bremsstrahlung. Th and U contents by EDXRF were out of interest. Other dashes mean lack of intensities of the corresponding  $K_{\alpha}$  lines to determine these lanthanides. Due to the high value of the ascribed expanded uncertainty  $U(C_a)$  in the interval of contents 20.0–49.9  $\mu\text{g g}^{-1}$ , several elements in Table 4 (Sm, Gd, Dy) and Table 5 (Eu, Ho), as well as Eu in Table 3, were analyzed semi-quantitatively ( $U(C_a)/C_a$  exceeds 30%).

To appraise consistency of the results of CRM analysis by EDXRF with the certified values ( $C_r$ ),  $E_n$ -score was assessed as a criterion recommended by IUPAC to verify laboratory performance [44]. All  $E_n$ -score numbers adduced in Tables 3, 4, 5 keep within the acceptable interval  $-1 < E_n < 1$  partly owing to high  $U(C_a)$  values mentioned above. However, taking that relative deviation  $(C_a - C_r)/C_r$  must be lower than 10%, Er in Table 4, Tb and Ho in Table 5 didn't pass  $E_n$ -score test. Hence, the corresponding results should be considered as indicative ones even despite Er and Tb were formally quantitatively determined.

On the other hand, allowable values of standard deviation of the results of element determination  $\sigma_{D,r}$  (in %) depending on the fixed intervals of contents are assigned by the basic document OST 41-08-212-04 regulating application

of analytical techniques for routine analysis of mineral resources [45]. For the lowest intervals  $\sigma_{D,r}$  doesn't exceed 30%, i.e. coincides with a requirement for the quantitative analysis. The other claim is insignificant values of the relative bias comparing with  $\sigma_{D,r}$  – they must be less than one third of the latter (the so-called criterion of “negligible inaccuracy”).

According to OST 41-08-212-04 the results of Er determination by EDXRF in OREAS 100a, Tb and Ho in OSO 528 must be excluded, as  $E_n$ -score test has shown before. Sm, Eu, Gd, and Dy passed the criterion of “negligible inaccuracy”, but these determinations should be considered semi-quantitative due to the high values of  $U(C_a)$ . As it was expected, the results of CRM analysis for Y and light lanthanides are acceptable.

A part of the X-ray spectrum of CRM OSO 528 counted for 45 min is shown in Fig. 1 as an example. In spite of the most intensive  $K_{\alpha 1}$  lines of Tb, Ho and Er are not too expressed, their intensities passed a statistical test laid in the software.

Comparing sensitivity of three CRM and common rock analysis for lanthanide contents [32], RLP-21T additionally enables to determine Eu in REE resources if its mass fraction exceeds that of UCC by one order of magnitude or more, Gd and Dy—if the excess is approximately fivefold. Because of the limited choice of the CRMs certified for REE high contents further discussion of sensitivity and accuracy of EDXRF is made comparing this method and INAA by the results of mineral resource analysis.

REE contents in three CRMs by comparator INAA with the corresponding  $E_n$ -score values are demonstrated in Tables 3, 4, 5 as well. Unlike EDXRF, almost all the elements of interest were determined except for Y. Mass fractions of Th and U causing the majority of spectral interferences were evaluated too. Expanded uncertainty of the INAA results was assessed following the expression published before [32, 37].

Peculiarities of OREAS 100a and OSO 528 analysis by comparator INAA have been already discussed rather explicitly [29]. In the present work Tables 4 and 5 comprise somewhere differing estimations since another approach was applied intended for REE determination in geological samples, not in specific objects like Zr concentrate.

Taking account of the high contents of light lanthanides in OREAS 460,  $m t_{irr}$  product showing its irradiation conditions was significantly diminished comparing with that for common rocks:  $m = 40$  mg and  $t_{irr} = 2$  h. Spectral interferences to La, Ce, and Nd analytical gamma-lines caused by the corresponding uranium fission products occurred far less 1% and hence were ignored. High count rate of Compton continuum in the vicinity of  $^{166}\text{Ho}$  gamma-line affected the accuracy of holmium determination since the contribution of  $^{133}\text{Xe}$  was evaluated approximately (about 15%). Intensive

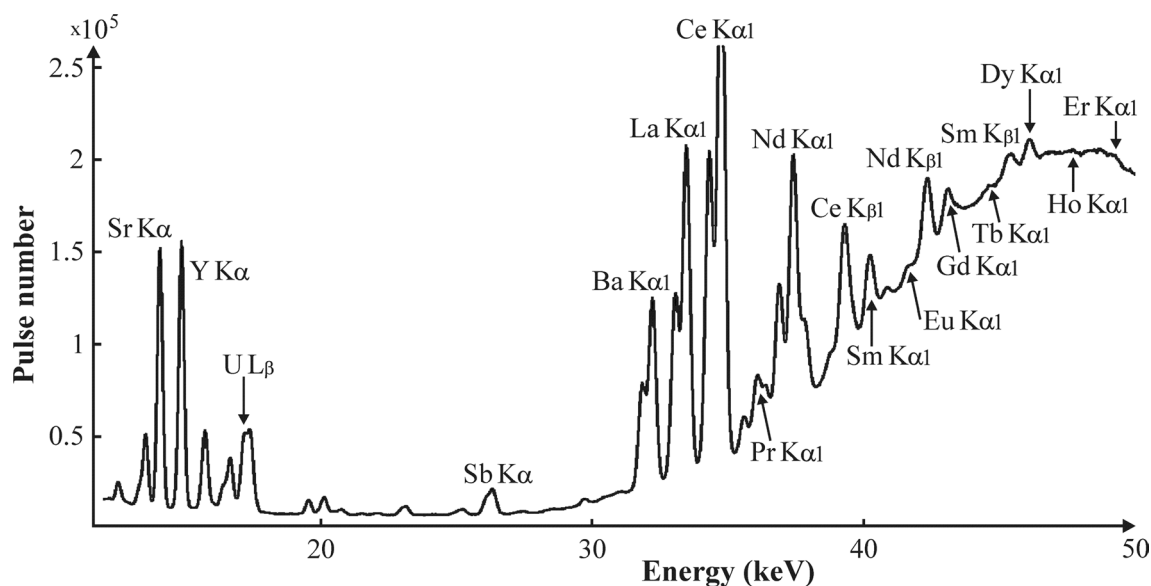


**Fig. 1** A part of the X-ray spectrum of CRM OSO 528

spectral interferences from  $^{233}\text{Pa}$  and  $^{182}\text{Ta}$  gamma-lines compelled to use the planar type SCD to determine Tb and Tm mass fractions, respectively. Contribution of  $^{233}\text{Pa}$  to the count rate of  $^{160}\text{Tb}$  analytical gamma-line came to  $\approx 3\%$ , while 85% of the count rate of  $^{170}\text{Tm}$  gamma-line was explained by the contribution of  $^{182}\text{Ta}$ . Accounted spectral interference of  $K_{\alpha 2}$  X-ray line of  $^{233}\text{Pa}$  to the count rate of  $^{165}\text{Dy}$  reached  $\approx 7\%$ . The gamma-line of  $^{161}\text{Tb}$  and  $K_{\alpha 1}$  X-ray line of Sn (resulting from  $^{122}\text{Sb}$  decay, Table 2) partially resolved by GLP36360 were divided by the software. Owing to the low mass fraction of Mn in OREAS 460 (about one third of its average crustal abundance  $1000 \mu\text{g g}^{-1}$  [38]), low content of Er in this CRM became accessible for evaluation.

All the results of CRM analysis for REE contents by INAA passed  $E_n$ -score test including relative deviations from the certified values which were overall  $< 10\%$ . The results also satisfy the requirements of OST 41-08-212-04 to the analytical techniques. Adequate accuracy of La and Th determination can be mentioned too to use them as the internal standards where necessary.

So, EDXRF and INAA being used together to analyze traditional rare earth resources, contents of all sixteen REE become accessible. Depending on their mass fractions, eight to eleven lanthanides plus Y can be determined by EDXRF quantitatively or semi-quantitatively. This offers the opportunity to combine the methods reasonably, i.e. to substitute INAA for far less laborious EDXRF where possible.

To verify this approach several ore samples collected from a ledge of Kundybai titanium-REE deposit, Northern Kazakhstan, were investigated at first. Rare earth elements of this large-scale field are mainly concentrated in argillaceous minerals associated with the Mesozoic weathering

crust of metamorphic rocks. The field differs favorably from the majority of other ones in the higher ratios of medium to light and heavy to light lanthanides [46].

The samples were measured for 60 min using RLP-21T; to conduct INAA for the long-lived radionuclides 100 mg assays (except for 30 mg one of sample 1120) were irradiated for 1 h, and for 3–5 min to determine Pr, Dy, and Er. REE contents of the Kundybai samples are presented in Table 6. Along with Th and U mass fractions as in the tables above, Mn contents by EDXRF and Na – by INAA are included taking account of their substantial effect on the sensitivity of Er and Pr determination by INAA, respectively.

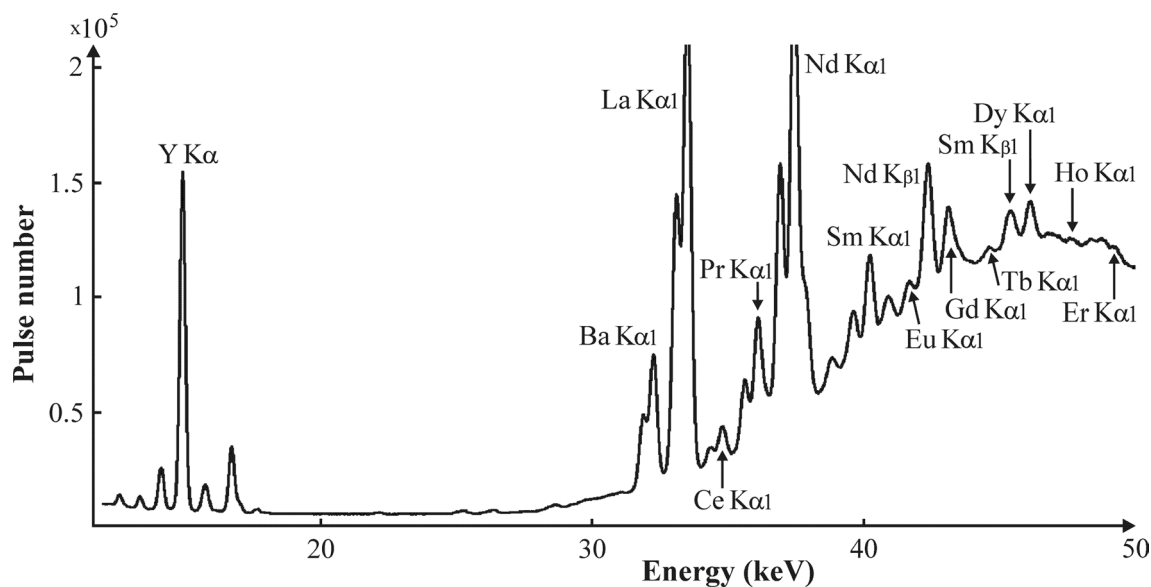
The lanthanide contents up to Er were evaluated quantitatively or semi-quantitatively by EDXRF. Unreliable assessments due to insufficient count rates of analytical X-ray lines were substituted for upper limits. EDXRF results basically coincide with that by INAA within a reasonable deviation  $\pm 10\%$  except for some Tb and Ho contents. These elements and probably Eu can be scarcely reliably determined by EDXRF in the selected samples using RLP-21T despite several successful coincidences with INAA results.

A part of X-ray spectrum of the most REE-rich sample is shown in Fig. 2. As the other ones except for 821, sample 1120 is characterized by low Ba content frequently impeding Pr determination in rocks (Table 1). Another peculiarity inherent to all five samples is sharp negative Ce anomaly resulted from the conditions of Kundybai formation. Therefore, to account correctly substantial spectral interference with  $^{175}\text{Yb}$ , Ce content was determined using the planar type SCD. Heavy lanthanide enrichment is most noticeable in samples 1119 and 1121; in terms of La/Yb ratio it reaches



**Table 6** REE and some other element contents of Kundybai deposit samples by EDXRF and INAA,  $\mu\text{g g}^{-1}$  ( $P=0.95$ )

| Element | 821       |           | 1119       |           | 1120       |           | 1121      |           | 1194      |           |
|---------|-----------|-----------|------------|-----------|------------|-----------|-----------|-----------|-----------|-----------|
|         | EDXRF     | INAA      | EDXRF      | INAA      | EDXRF      | INAA      | EDXRF     | INAA      | EDXRF     | INAA      |
| Sc      | –         | 34.2±3.4  | –          | 45.2±4.5  | –          | 44.2±4.4  | –         | 50.7±5.0  | –         | 52.2±5.2  |
| Y       | 186±23    | –         | 560±100    | –         | 690±100    | –         | 322±48    | –         | 289±48    | –         |
| La      | 214±48    | 220±22    | 250±48     | 238±24    | 840±100    | 859±86    | 222±48    | 221±22    | 214±48    | 217±21    |
| Ce      | 68±13     | 68.3±6.8  | 21.0±8.3   | 21.7±2.2  | 56±13      | 56.4±5.6  | 22.4±8.3  | 23.4±2.3  | 21.6±8.3  | 20.4±2.0  |
| Pr      | 42.0±8.3  | 42.6±4.3  | 65±13      | 65.9±6.6  | 203±48     | 221±22    | 50±13     | 50.6±5.1  | 45.5±8.3  | 47.6±4.8  |
| Nd      | 174±23    | 168±17    | 294±48     | 289±28    | 920±100    | 963±96    | 237±48    | 242±24    | 207±48    | 204±20    |
| Sm      | 34.7±8.3  | 34.6±3.5  | 91±13      | 87.6±8.8  | 276±48     | 270±27    | 75±13     | 76.2±7.6  | 52±13     | 48.9±4.9  |
| Eu      | <10       | 8.07±0.81 | 25.9±8.3   | 26.6±2.7  | 86±13      | 84.9±8.5  | 22.8±8.3  | 23.8±2.4  | <10       | 13.2±1.3  |
| Gd      | 31.2±8.3  | 31.5±3.2  | 83±13      | 81.4±8.1  | 237±48     | 246±25    | 82±13     | 81.6±8.2  | 55±13     | 55.4±5.5  |
| Tb      | <10       | 5.31±0.53 | 16.3±4.4   | 17.9±1.8  | 40.2±8.3   | 44.2±4.3  | 13.9±4.4  | 14.8±1.5  | 10.3±4.4  | 8.29±0.83 |
| Dy      | 29.2±8.3  | 30.1±3.0  | 118±23     | 125±12    | 235±48     | 231±2.3   | 89±13     | 85.4±8.5  | 48.2±8.3  | 50.0±5.0  |
| Ho      | <10       | 5.52±0.65 | 29.2±8.3   | 23.9±2.6  | 46.8±8.3   | 48.9±4.9  | 22.2±8.3  | 15.0±1.8  | 15.6±4.4  | 9.1±1.0   |
| Er      | <10       | 15.9±1.6  | 67±13      | 70.2±7.0  | 125±23     | 116±12    | 47.6±8.3  | 48.9±4.9  | 28.1±8.3  | 30.0±3.0  |
| Tm      | –         | 2.18±0.23 | –          | 9.02±0.90 | –          | 15.8±1.6  | –         | 6.57±0.66 | –         | 3.84±0.38 |
| Yb      | –         | 14.2±1.4  | –          | 61.6±6.2  | –          | 106±11    | –         | 46.5±4.6  | –         | 24.0±2.4  |
| Lu      | –         | 2.02±0.21 | –          | 8.95±0.90 | –          | 14.7±1.5  | –         | 6.74±0.67 | –         | 3.73±0.37 |
| Th      | –         | 5.00±0.50 | –          | 1.17±0.15 | –          | 1.1±0.3   | –         | 1.70±0.20 | –         | 1.44±0.18 |
| U       | –         | 2.6±0.5   | –          | <1        | –          | <1        | –         | <1        | –         | <1        |
| Mn      | 1490±200  | –         | 1770±200   | –         | 2260±480   | –         | 930±100   | –         | 1230±200  | –         |
| Na, %   | –         | 0.31±0.03 | –          | 0.61±0.06 | –          | 0.83±0.08 | –         | 0.42±0.04 | –         | 0.56±0.06 |
| Fe, %   | 9.27±0.30 | –         | 12.22±0.45 | –         | 11.30±0.45 | –         | 9.38±0.30 | –         | 9.57±0.30 | –         |

**Fig. 2** A part of X-ray spectrum of sample 1120 (Kundybai)

$\approx 3.9$  and  $\approx 4.8$ , respectively, comparing with the value for the UCC (12.2).

On the whole, apart from Mn increased contents (bringing to decay time extension by one half-life of  $^{56}\text{Mn}$ ), elemental composition of the samples including low mass

fractions of Ba, Na, Th, and U and high contents of Fe is favorable enough to conduct both EDXRF and comparator INAA. The methods can be integrated as follows: Y, La to Sm, Gd, Dy, and most often Er are determined by EDXRF, the other seven REEs – by INAA. Main advantage consists

**Table 7** REE and some other element contents of Shok-Karagai deposit samples by EDXRF and INAA,  $\mu\text{g g}^{-1}$  ( $P=0.95$ )

| Element | 7004/10  |             | 7005/14     |           | 7007/11  |             | 5005/8    |           | 5006/10   |           |
|---------|----------|-------------|-------------|-----------|----------|-------------|-----------|-----------|-----------|-----------|
|         | EDXRF    | INAA        | EDXRF       | INAA      | EDXRF    | INAA        | EDXRF     | INAA      | EDXRF     | INAA      |
| Sc      | –        | 1.96±0.20   | –           | 3.52±0.35 | –        | 2.79±0.28   | –         | 38.0±3.8  | –         | 62.6±6.2  |
| Y       | 348±48   | –           | 384±48      | –         | 360±48   | –           | 128±23    | –         | 371±48    | –         |
| La      | 810±100  | 796±80      | 404±48      | 396±40    | 730±100  | 730±74      | 105±23    | 106±11    | 168±23    | 164±16    |
| Ce      | 500±100  | 508±51      | 244±48      | 238±24    | 550±100  | 569±57      | 98±13     | 102±10    | 271±48    | 280±28    |
| Pr      | 110±23   | 116±12      | 65±13       | 64.9±6.5  | 134±23   | 140±14      | 31.7±8.3  | 31.3±3.8  | 43.7±8.3  | 45.6±4.6  |
| Nd      | 422±48   | 417±42      | 244±48      | 239±24    | 499±48   | 510±51      | 153±23    | 158±16    | 211±23    | 212±21    |
| Sm      | 81±13    | 81.8±8.2    | 46.6±8.3    | 47.5±4.8  | 93±13    | 95.3±9.5    | 43.1±8.3  | 42.3±4.2  | 60±13     | 59.2±5.9  |
| Eu      | –        | 3.31±0.33   | –           | 2.64±0.26 | –        | 5.83±0.58   | <10       | 9.90±1.0  | 14.0±4.4  | 14.0±1.4  |
| Gd      | 85±13    | 80.4±8.1    | 49.9±8.3    | 49.1±5.0  | 82±13    | 80.9±8.2    | 38.9±8.3  | 39.6±4.0  | 66±13     | 63.1±6.3  |
| Tb      | 11.5±4.4 | 12.5±1.3    | <10         | 8.82±0.88 | 12.7±4.4 | 12.4±1.2    | <10       | 5.45±0.54 | 10.9±4.4  | 10.2±1.0  |
| Dy      | 59±13    | 59.9±6.0    | 47.4±8.3    | 50.1±5.0  | 62±13    | 60.9±6.1    | 26.4±8.3  | 26.7±2.8  | 60±13     | 61.0±6.1  |
| Ho      | 13.7±4.4 | 11.2±1.3    | 16.7±4.4    | 10.7±1.3  | 17.8±4.4 | 15.3±1.8    | <10       | 5.23±0.63 | 18.5±4.4  | 13.6±1.4  |
| Er      | 24.4±8.3 | 25.2±2.7    | 36.1±8.3    | 35.3±3.5  | 35.5±8.3 | 34.5±3.5    | <15       | 15.6±1.7  | 36.8±8.3  | 37.4±3.7  |
| Tm      | –        | 3.52±0.36   | –           | 5.01±0.50 | –        | 4.40±0.44   | –         | 2.45±0.25 | –         | 5.44±0.55 |
| Yb      | –        | 19.5±2.0    | –           | 35.3±3.5  | –        | 30.4±3.0    | –         | 16.4±1.6  | –         | 37.6±3.8  |
| Lu      | –        | 2.41±0.24   | –           | 4.77±0.48 | –        | 3.92±3.9    | –         | 2.52±0.25 | –         | 5.60±0.56 |
| Th      | –        | 57.7±5.8    | –           | 66.1±6.6  | –        | 71.6±7.2    | –         | 2.43±0.24 | –         | 1.6±0.2   |
| U       | –        | 14.2±1.5    | –           | 11.7±1.2  | –        | 13.0±1.3    | –         | 2.3±0.7   | –         | 2.3±0.7   |
| Mn      | <100     | –           | 110±23      | –         | <100     | –           | 1360±200  | –         | 830±100   | –         |
| Na, %   | –        | 2.32±0.23   | –           | 1.49±0.15 | –        | 1.43±0.14   | –         | 0.90±0.09 | –         | 0.40±0.04 |
| Fe, %   | –        | 0.872±0.087 | 1.915±0.081 | –         | –        | 0.867±0.087 | 6.74±0.30 | –         | 4.98±0.17 | –         |

in the absence of time-consuming evaluation of Pr and Er mass fractions by INAA. Moreover, GLP36360 can be excluded due to negligible corrections to  $^{166}\text{Ho}$  count rates in view of low U contents.

As another example, several ore samples collected from two different sites of Shok-Karagai REE deposit (Syrymbet ore province, Northern Kazakhstan) were selected. The field presented by Cenozoic weathering crusts is analogous to Kundybai genetically. Large REE resources are associated with ionic clays, complex rare metal and rare earth mineralization [47]. Light lanthanides predominate in the deposit accompanied by Th increased contents.

100 mg of each sample were irradiated for 1 h and for 4–5 min to conduct INAA for the long-lived and short-lived radionuclides, respectively. The determined REE contents together with EDXRF results and other data are summarized in Table 7. The two sites differ noticeably in their Th and U mass fractions as well as in macro-component composition. This affected INAA carrying out—particularly, lower Fe contents in 7004/10 and 7007/11 were more precisely determined by INAA, and Th was used as the internal standard to analyze the samples for Gd and Ho. In the rest, INAA of the samples was carried out following the procedure above. Contribution of U fission products was very small, less 1% and less 3% to the count rates of  $^{147}\text{Nd}$  and  $^{141}\text{Ce}$ , respectively. Correction for  $^{182}\text{Ta}$  count rate (Tm determination)

was rather moderate too about 13–16% for the first three samples. The other ones from the second site didn't require this correction at all.

EDXRF of the Shok-Karagai samples was complicated by nothing including low Ba contents less than  $250 \mu\text{g g}^{-1}$ . Table 7 data can be used to evaluate lower limit of semi-quantitative analysis of the samples for Er mass fraction—about  $20 \mu\text{g g}^{-1}$ . As for Kundybai deposit, the problem of Eu, Tb and Ho determination arose due to insufficient sensitivity and reliability of the method for these intervals of contents. The other EDXRF results are in good agreement with INAA. So, recommendation on combination of these two methods is the same as above.

Table 8 presents the results of REE determination in the samples collected from the large rare metal field Upper Espe in Zharma-Saur belt, East Kazakhstan, characterized by diverse metallogenic types. Rare earths are associated with alkaline and sub-alkaline granites corresponding to Permian intrusions [46]. Owing to vast prevalence of Y group REEs, as well as to accompanying complex Be–Nb–Ta mineralization, the deposit belongs to the most promising ones in the country.

Due to the great difference in REE contents of the material selected from an ore body and the bearing strata revealed by EDXRF, 100 mg assay (samples s4 and s5) was drastically reduced for the other samples down to 2.6 mg (s2k), and

**Table 8** REE and some other element contents of Upper Espe deposit samples by EDXRF and INAA,  $\mu\text{g g}^{-1}$  ( $P=0.95$ )

| Element | s1k             |                 | s2k              |                 | s3              |                 | s4              |                 | s5                |                 |
|---------|-----------------|-----------------|------------------|-----------------|-----------------|-----------------|-----------------|-----------------|-------------------|-----------------|
|         | EDXRF           | INAA            | EDXRF            | INAA            | EDXRF           | INAA            | EDXRF           | INAA            | EDXRF             | INAA            |
| Sc      | –               | $5.40 \pm 0.54$ | –                | $9.77 \pm 0.98$ | –               | $0.56 \pm 0.06$ | –               | $0.83 \pm 0.08$ | –                 | $0.57 \pm 0.06$ |
| Y       | $2010 \pm 480$  | –               | $10,470 \pm 810$ | –               | $192 \pm 23$    | –               | $101 \pm 23$    | –               | $101 \pm 23$      | –               |
| La      | $151 \pm 23$    | $156 \pm 15$    | $590 \pm 100$    | $584 \pm 58$    | $90 \pm 13$     | $91.6 \pm 9.1$  | $41.7 \pm 8.3$  | $43.5 \pm 4.3$  | $67 \pm 13$       | $66.6 \pm 6.7$  |
| Ce      | $373 \pm 48$    | $382 \pm 38$    | $1730 \pm 200$   | $1660 \pm 160$  | $255 \pm 48$    | $263 \pm 26$    | $140 \pm 23$    | $147 \pm 15$    | $197 \pm 23$      | $203 \pm 20$    |
| Pr      | $59 \pm 13$     | –               | $270 \pm 48$     | $284 \pm 28$    | $34.0 \pm 8.3$  | –               | $14.9 \pm 4.4$  | –               | $22.5 \pm 8.3$    | –               |
| Nd      | $261 \pm 48$    | $262 \pm 26$    | $1260 \pm 200$   | $1260 \pm 120$  | $119 \pm 23$    | $127 \pm 13$    | $64 \pm 13$     | $68.6 \pm 6.9$  | $91 \pm 13$       | $94.6 \pm 9.5$  |
| Sm      | $173 \pm 23$    | $167 \pm 17$    | $890 \pm 100$    | $873 \pm 87$    | $51 \pm 13$     | $51.1 \pm 5.0$  | $32.1 \pm 8.3$  | $32.2 \pm 3.2$  | $35.0 \pm 8.3$    | $35.3 \pm 3.5$  |
| Eu      | –               | $2.60 \pm 0.26$ | <10              | $13.3 \pm 1.3$  | –               | $0.78 \pm 0.08$ | –               | $0.44 \pm 0.05$ | –                 | $0.45 \pm 0.05$ |
| Gd      | $206 \pm 48$    | $199 \pm 20$    | $1160 \pm 200$   | $1210 \pm 140$  | $41.6 \pm 8.3$  | $43.3 \pm 4.3$  | $33.6 \pm 8.3$  | $34.1 \pm 3.4$  | $34.8 \pm 8.3$    | $33.6 \pm 3.6$  |
| Tb      | $52 \pm 13$     | $60.5 \pm 6.1$  | $276 \pm 48$     | $292 \pm 29$    | <10             | $9.40 \pm 0.90$ | <10             | $6.93 \pm 0.68$ | <10               | $5.52 \pm 0.55$ |
| Dy      | $417 \pm 48$    | $440 \pm 45$    | $2150 \pm 480$   | $2200 \pm 220$  | $44.2 \pm 8.3$  | $43.3 \pm 4.3$  | $31.5 \pm 8.3$  | $30.4 \pm 3.2$  | $24.7 \pm 8.3$    | $25.1 \pm 2.5$  |
| Ho      | $103 \pm 23$    | $101 \pm 12$    | $570 \pm 100$    | $550 \pm 55$    | <10             | $10.5 \pm 1.2$  | <10             | $6.62 \pm 0.70$ | <10               | $5.08 \pm 0.56$ |
| Er      | $296 \pm 48$    | $303 \pm 30$    | $1500 \pm 200$   | $1450 \pm 140$  | $26.7 \pm 8.3$  | $27.7 \pm 4.0$  | <15             | $10 \pm 4$      | <15               | <10             |
| Tm      | –               | $58.8 \pm 5.9$  | –                | $173 \pm 17$    | –               | $4.83 \pm 0.48$ | –               | $2.34 \pm 0.23$ | –                 | $1.21 \pm 0.13$ |
| Yb      | $510 \pm 100$   | $519 \pm 50$    | $1080 \pm 200$   | $1060 \pm 100$  | –               | $33.7 \pm 3.3$  | –               | $18.8 \pm 1.9$  | –                 | $7.29 \pm 0.73$ |
| Lu      | –               | $91.1 \pm 9.0$  | –                | $128 \pm 12$    | –               | $5.03 \pm 0.50$ | –               | $3.00 \pm 0.30$ | –                 | $1.09 \pm 0.10$ |
| Th      | –               | $1630 \pm 160$  | –                | $213 \pm 21$    | –               | $52.3 \pm 5.2$  | –               | $72.3 \pm 7.2$  | –                 | $22.5 \pm 2.2$  |
| U       | –               | $10.2 \pm 1.2$  | $17.4 \pm 4.4$   | –               | –               | $17.7 \pm 1.7$  | –               | $12.9 \pm 1.3$  | –                 | $3.1 \pm 0.3$   |
| Mn      | $2110 \pm 480$  | –               | $1660 \pm 200$   | –               | $530 \pm 100$   | –               | $590 \pm 100$   | –               | $510 \pm 100$     | –               |
| Na, %   | –               | $4.51 \pm 0.45$ | –                | $5.43 \pm 0.54$ | –               | $4.55 \pm 0.45$ | –               | $3.50 \pm 0.35$ | –                 | $3.45 \pm 0.35$ |
| Fe, %   | $3.66 \pm 0.17$ | –               | $3.40 \pm 0.17$  | –               | $2.11 \pm 0.17$ | –               | $2.33 \pm 0.17$ | –               | $1.614 \pm 0.081$ | –               |

irradiation conditions were changed from 250 to 6.5 mg h ( $t_{irr} = 2.5$  h) in terms of  $m t_{irr}$  product. In case of short irradiation  $m t_{irr}$  varied less abruptly within 50–400 mg min.

The tiny mass of s2k assay ensured the value of neutron flux self-shielding 2–2.5% assessed by the spreadsheet [42], which can be ignored. This quantity is far less the most typical one (about 100 mg) used for rock sample analysis [7], hence the problem of very small assay representativeness remains in abeyance. In the present instance several mg of the mass are seemingly still representative of the bulk sample owing to its fine grinding by the client. Good comparability of EDXRF and INAA results noted below can serve as an indirect confirmation of this assumption.<sup>3</sup> However, the situation can change in the case of less careful grinding or another mineral composition of the samples, more resistant to milling. So, investigating very small assays of geological samples by INAA, several replicas are recommended in general.

On the other hand,  $^{59}\text{Fe}$  count rate became evidently insufficient to use Fe as the internal standard, so the method

of “external addition” of the comparator was applied [37] to calculate REE contents of samples s1k and s2k.

Among the other samples, the ore one s1k is characterized by REE ratios most far from that for UCC and by the highest Th content, hence by the largest spectral interferences caused by  $^{233}\text{Pa}$ . Accounted contribution of the latter to the count rates of  $^{160}\text{Tb}$  and  $^{165}\text{Dy}$  gamma-lines amounted  $\approx 3.5\%$  and approached 9%, respectively. About 12% of the  $^{141}\text{Ce}$  analytical peak area was explained by contribution of  $^{175}\text{Yb}$ . Correction to  $^{170}\text{Tm}$  gamma-line count rate was rather moderate, about 3.7%, but reached 22–26% for the other samples except for s2k (which didn't need it). Intensive Compton continuum caused by Na high contents prevented Pr determination in all samples except for the richest amount in s2k. On the whole, due to the complicated composition, INAA of the Upper Espe samples turned into a rather laborious procedure.

By contrast to this, the object is favorable to conduct EDXRF including low Ba mass fractions no more than  $150 \mu\text{g g}^{-1}$ . High Yb contents became available for determination in two ore samples s1k and s2k. Expressed X-ray peaks of Yb, including interference free  $K_{\alpha 2}$  line to the left of  $K_{\alpha 1}$  one in Fig. 3, presenting a part of the X-ray spectrum of sample s1k, point out that quantitative analysis of Yb using RLP-21T can be carried out beginning from a half content in sample s1k, at least.

<sup>3</sup> Conducting EDXRF by RLP-21 T, the rock sample mass depending on the maximum escape depth of the characteristic X-rays of the lanthanides is several g.

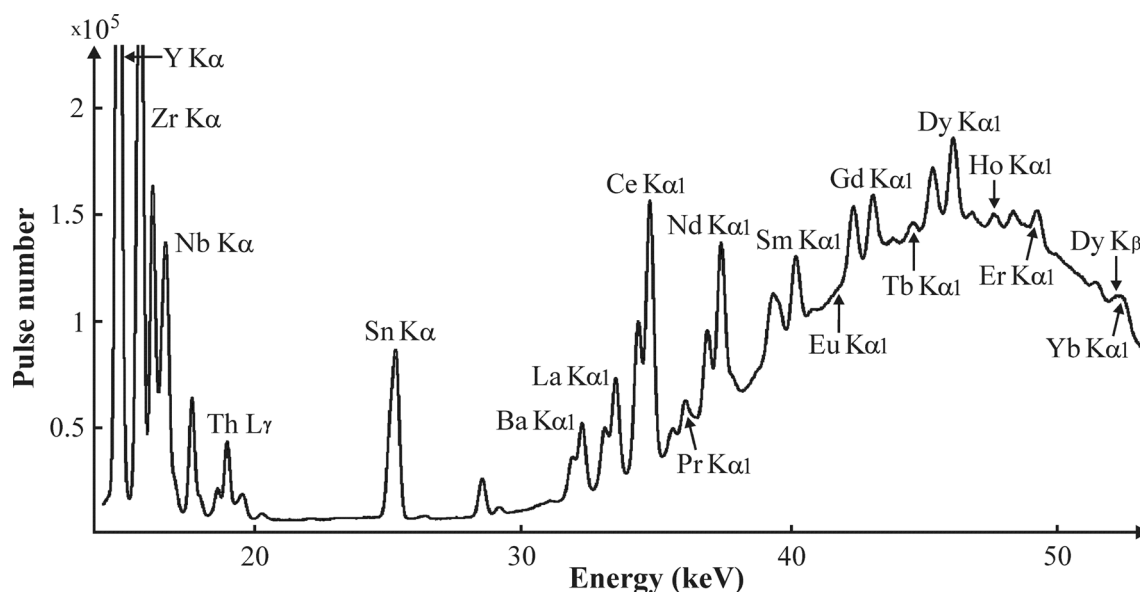


**Fig. 3** A part of the X-ray spectrum of sample 1 k (Upper Espe)

Collation with UNAA results, where possible, showed a comparable pattern as in the previous examples except for sample 1k analysis for Tb content. So, keeping to the way of two method integration on the whole, Ho and Yb can be evidently additionally determined by EDXRF in the ore samples considerably enriched with heavy REEs like in Upper Espe. It's difficult to assert the same about Tb since the number of the studied samples characterized by its high contents was insufficient.

## Conclusions

Joint application of comparator INAA and EDXRF was considered to determine all sixteen available REEs in corresponding mineral resources, while eight to eleven lanthanides were determined by both methods depending on their contents. Apart from INAA, this became possible owing to the new capacities of the modified version of portable EDXRF spectrometer RLP-21T which was specially designed to analyze geological samples for lanthanide contents by K series of their characteristic X-rays.

Analyzing the samples from three REE fields of different types from a usual one, characterized by significant predominance of light lanthanides, to a deposit greatly enriched with the heavy REEs, advantages and drawbacks of the two methods were revealed. Despite the apparent benefit of K series excitation, RLP-21T implements rather prompt but still less sensitive and reliable determination of medium and heavy lanthanides comparing with INAA. Tm is left inaccessible due to the low count rate of its K lines against the unfavorable peak-to-background ratio. The same concerns

Lu, but mainly due to insufficient voltage at the X-ray tube to produce intensive high-energy bremsstrahlung. Yb can be measured reliably beginning from its high mass fractions of several hundreds  $\mu\text{g g}^{-1}$  only.

All REEs except for Y may be determined in principle by INAA in REE mineral resources. In case of REE higher contents count rates of the low-energy (25.65 keV) gamma-line of  $^{161}\text{Tb}$  become sufficient to determine Gd using a planar-type SCD. This makes possible to reduce the time of REE analysis by a fortnight approximately, comparing with the traditional measuring of  $^{153}\text{Gd}$  after more than a month of decay. Reliability of Gd determination can be also improved since REE ores are often accompanied by Th high contents resulting in serious spectral interferences of  $^{233}\text{Pa}$  to the analytical gamma-lines of  $^{153}\text{Gd}$ . Moreover, in this case Th can serve as an internal standard too [35]. However, still far longer time and greater cost of INAA remain its main disadvantages. Determination of high REE mass fractions in complicated objects is rather laborious, needs the additional equipment and a qualified personnel. Besides, sensitivity of Pr and Er determination depends on elemental composition of the samples, mainly on Na and Mn contents.

Based on the present investigation, the next way to combine the methods to analyze REE ores can be proposed, if necessary equipment is available. Just like the usual rock investigation [32], EDXRF is used first to determine the contents of Y and light lanthanides (La to Sm), as well as Gd, Dy and Er (the last one where possible). Mass fractions of the other seven REEs are measured by INAA, all by the long-lived radionuclides. Necessity of the additional short-time irradiation appears basically in the case of Er determination, if its content is inaccessible authentically by EDXRF.

Pr and Dy, as a rule, can be reliably measured in REE ores by their characteristic X-rays. Further development of the approach could take place if a higher voltage model of the X-ray tube would be installed in RLP-21T.

**Acknowledgements** The work was supported by a grant from Ministry of Education and Sciences of the Republic of Kazakhstan (BR23891691).

## Declarations

**Conflict of interest** The author has no competing interests to declare that are relevant to the content of this article.

## References

- Inobeme A, Mathew JT, Jatto E et al (2023) Recent advances in instrumental techniques for heavy metal quantification. *Environ Monit Assess.* <https://doi.org/10.1007/s10661-023-11058-3>
- Balaram V (2023) Advances in analytical techniques and applications in exploration, mining, extraction, and metallurgical studies of rare earth elements. *Minerals.* <https://doi.org/10.3390/min13081031>
- Zuma MC, Lakkakula J, Mketi N (2022) Recent trends in sample preparation methods and plasma-based spectrometric techniques for the determination of rare earth elements in geological and fossil fuel samples. *Appl Spectrosc Rev* 57:353–377
- El-TaHER A (2018) Nuclear analytical techniques for detection of rare earth elements. *J Rad Nucl Appl* 3:53–64
- Schramm R (2016) Use of X-ray fluorescence analysis for the determination of rare earth elements. *Phys Sci Rev.* <https://doi.org/10.1515/psr-2016-0061>
- Balaram V, Subramanyam KSV (2022) Sample preparation for geochemical analysis: Strategies and significance. *Adv Sample Prepar.* <https://doi.org/10.1016/j.sampre.2022.100010>
- Stosch H-G (2016) Neutron activation analysis of the rare earth elements (REE) – with emphasis on geological materials. *Phys Sci Rev.* <https://doi.org/10.1515/psr-2016-0062>
- Folkedahl B, Nyberg C, Biswas S et al (2023) Round-robin inter-laboratory study on rare-earth elements in US-based geologic materials. *Minerals.* <https://doi.org/10.3390/min13070944>
- Attallah MF, Abdou FS, Aly HF (2021) Microanalysis and signature of rare earth elements in geochemical samples using neutron activation analysis. *Radiochim Acta* 109:225–232
- Marques R, Prudêncio MI, Russo D (2021) Rare earths and other chemical elements determined by neutron activation analysis in new reference USGS materials: carbonatite, nephelinite, syenite, granite, stream sediment and marine shale. *J Radioanal Nucl Chem* 327:1229–1236
- Ashraf A, Saion E, Gharibshahi E et al (2016) Rare earth elements in core marine sediments of coastal East Malaysia by instrumental neutron activation analysis. *Appl Radiat Isot* 107:17–23
- Santoro A, Thoss V, Guevara SR et al (2016) Assessing rare earth elements in quartz rich geological samples. *Appl Radiat Isot* 107:323–329
- X-ray Transition Energies Database. <https://www.nist.gov/pml/x-ray-transition-energies-database>. Accessed 15 March 2024
- Karivai A, Zuzaan P, Gustova V (2011) A method for the determination of some rare earth elements and their correlation with thorium using X-ray fluorescence. *Phys Part Nucl Lett* 6:576–580
- Cojocar V, Pantelic A, Pincovschi E et al (2006) EDXRF versus INAA in a pollution control of soil. *J Radioanal Nucl Chem* 268:71–78
- Savichev AT, Vodyanitskii YuN (2012) Improvement of the X-ray radiometric method of lanthanide diagnostics in soils. *Eurasian Soil Sci* 45:665–674
- Margu E, Queral I, de Almeida E (2022) X-ray fluorescence spectrometry for environmental analysis: Basic principles, instrumentation, applications and recent trends. *Chemosphere.* <https://doi.org/10.1016/j.chemosphere.2022.135006>
- Silva CD, Santana GP, Paz SPA (2020) Determination of La, Ce, Nd, Sm, and Gd in mineral waste from cassiterite beneficiation by wavelength-dispersive X-ray fluorescence spectrometry. *Talanta.* <https://doi.org/10.1016/j.talanta.2019.120254>
- Panchuk V, Yaroshenko I, Legin A et al (2018) Application of chemometric methods to XRF-data—a tutorial review. *Anal Chim Acta* 1040:19–32
- Smoliński A, Stępin M, Howaniec N (2016) Determination of rare earth elements in combustion ashes from selected Polish coal mines by wavelength dispersive X-ray fluorescence spectrometry. *Spectrochim Acta Part B* 116:63–74
- Sá ÍP, Almeida ON, Lima DDC et al (2021) Determination of lanthanide and actinide elements by energy dispersive x-ray fluorescence spectrometry applying DLLME preconcentration and dried spot. *Spectrochim Acta, Part B.* <https://doi.org/10.1016/j.sab.2021.106253>
- Silachyov I, Akymbek Y (2023) Element content of the samples of medieval ceramics from Southern Kazakhstan: searching the way of preliminary differentiation. *J Radioanal Nucl Chem* 332:3799–3811
- Li C, Hu H, Yang MF et al (2022) Characteristics of the lunar samples returned by the Chang'E-5 mission. *Natl Sci Rev.* <https://doi.org/10.1093/nsr/nwab188>
- Chand M, Senthilvadivu R, Rao JSB et al (2020) Elemental characterization of coal fly ash using  $k_0$ -based IM-NAA and EDXRF towards its potential utilization and environmental concern. *J Radioanal Nucl Chem* 324:1089–1097
- Dasari KB, Cho H, Jacimovic R et al (2020) Chemical composition of asian dust in Daejeon, Korea, during the spring season. *ACS Earth and Space Chem* 4:1227–1236
- Rocha FR, Silva PS, Castro LM et al (2015) NAA and XRF technique bottom sediment assessment for major and trace elements: Tietê River, São Paulo State, Brazil. *J Radioanal Nucl Chem* 306:655–665
- Baljinyam N, Davaasuren B, Norov N et al (2015) Determination of rare earths and other trace elements in ore samples of Mongolia by WDXRF and INAA. *Физик ээргүүл* 20:51–54
- Abisheva ZS, Karshigina ZB, Bochevskaya YG et al (2017) Recovery of rare earth metals as critical raw materials from phosphorus slag of long-term storage. *Hydrometallurgy* 173:271–282
- Silachyov I (2023) Zircon concentrate analysis for sixteen rare earth elements by the complex of nuclear analytical methods. *J Radioanal Nucl Chem* 332:2017–2026
- Badawy W, Silachyov I, Dmitriev A et al (2023) Elemental distribution patterns in rock samples from Egypt using neutron activation and complementary X-ray fluorescence analyses. *Appl Radiat Isot.* <https://doi.org/10.1016/j.apradiso.2023.111063>
- Silachyov IYu (2018) Determination of rare earths in uranium raw material by neutron activation analysis and X-ray fluorescence. *News Acad Sci RK, Ser Chem Technol* 429(3):28–38
- Silachyov IYu (2020) Combination of neutron activation analysis with X-ray fluorescence spectrometry for the determination of rare-earth elements in geological samples. *J Anal Chem* 75:878–889
- Kortright JB, Thompson AC (2009) X-ray emission energies. In: Thompson AC (ed) X-ray data booklet, LBNL, Berkeley
- Rizo OD, Alvarez I, Herrera E et al (1997) HAV-I: A multipurpose multimonitor for reactor neutron flux characterization. *J Radioanal Nucl Chem* 220:99–102

35. Silachyov IYu (2020) Using the internal standard method with a planar detector in the determination of lanthanides in geological samples by neutron activation analysis. *J Anal Chem* 75:1415–1423
36. Ismail SS (2010) A new automated sample transfer system for instrumental neutron activation analysis. *J Autom Methods Manage Chem*. <https://doi.org/10.1155/2010/389374>
37. Silachyov I (2020) Elemental analysis of vegetation samples by INAA internal standard method. *J Radioanal Nucl Chem* 324:97–108
38. Rudnick RL, Gao S (2014) Composition of the continental crust. In: Holland HD, Turekian KK (eds) *Treatise on geochemistry*, vol 4, 2nd edn. Elsevier, Amsterdam
39. K0-Neutron activation analysis link page. The NDC k0-database 2019. <http://www.kayzero.com/k0naa/k0naaorg/Links.html>. Accessed 15 March 2024
40. Greenberg RR, Bode P, Fernandes EA (2011) Neutron activation analysis: a primary method of measurement. *Spectrochim Acta Part B* 66:193–241
41. Shirai N, Hidaka Y, Yamaguchi A et al (2015) Neutron activation analysis of iron meteorites. *J Radioanal Nucl Chem* 303:1375–1380
42. Chilian C, St-Pierre J, Kennedy G (2008) Complete thermal and epithermal neutron selfshielding corrections for NAA using a spreadsheet. *J Radioanal Nucl Chem* 278:745–749
43. Arbocò FF, Vermaercke P, Verheyen L et al (2014) Experimental evaluation of epithermal neutron self-shielding for  $^{96}\text{Zr}$  and  $^{98}\text{Mo}$ . *J Radioanal Nucl Chem* 297:371–375
44. ISO 13528:2022 (2022) *Statistical Methods for Use in Proficiency Testing by Interlaboratory Comparisons*. Genève, Switzerland
45. Gusev S, Ryabev V, Vorob'yov V, et al (2004) OST 41-08-212-04 Industrial Standard. Quality management of analytical work. Error guidelines for chemical analysis of mineral resources and precision classification of laboratory analytical techniques. Published by FSMC VIMS, Moscow (in Russian)
46. Petrov OV, Morozov AF, Kiselev EA, et al (ed) (2017) *Metallogeny of Northern, Central and Eastern Asia*. VSEGEI Printing House, St. Petersburg
47. Togizov K, Issayeva L, Muratkhonov D et al (2023) Rare earth elements in the Shok-Karagay ore fields (Syrymbet ore district Northern Kazakhstan) and visualisation of the deposits using the geography information system. *Minerals*. <https://doi.org/10.3390/min13111458>

**Publisher's Note** Springer Nature remains neutral with regard to jurisdictional claims in published maps and institutional affiliations.

Springer Nature or its licensor (e.g. a society or other partner) holds exclusive rights to this article under a publishing agreement with the author(s) or other rightsholder(s); author self-archiving of the accepted manuscript version of this article is solely governed by the terms of such publishing agreement and applicable law.